Conductivity of coupled quantum wells under an in-plane magnetic field

O. E. Raichev and F. T. Vasko
Institute of Semiconductor Physics, National Academy of Sciences of the Ukraine, Prospekt Nauki 45, Kiev-28, 252650, Ukraine
(Received 2 June 1995; revised manuscript received 26 July 1995)

The electrical conductivity tensor of the double quantum wells in the magnetic field parallel to the layers is calculated. The system of kinetic equations for the tunnel-coupled electron states is analyzed for the case of elastic scattering. The anisotropic suppression of the tunnel coupling and deformation of the Fermi surface by the magnetic field give rise to the complex magnetic field dependence of the conductivity tensor. The anisotropy of conductivity, as well as the negative magnetoresistance due to suppression of the resonant tunnel coupling in the structures with nonsymmetrical distributions of scatterers, are described. The results of the calculations are in agreement with the experimental data.

I. INTRODUCTION

Modifications of the electron energy spectrum in a single quantum well under a magnetic field parallel to the two-dimensional (2D) layer (in-plane magnetic field), such as shift of the levels and anisotropic dependence of the energy upon the 2D momentum $\mathbf{p}$, are significant only in the case of very strong fields, when the cyclotron energy $\hbar\omega_c$ is comparable with the size quantization energy.[1] However, in the double quantum wells (DQW's) with tunnel-coupled electron states, the modifications of the electron spectrum are considerable even in the fields as low as 1 T.[2,3] To understand the reason for this difference, it is necessary to take into account that the magnetic field deflects motion of the electrons and drives the tunnel-coupled states out of the tunneling resonance. Such an effect is significant when the energy $\varepsilon_H = \hbar\omega_c Z/\lambda$, where λ is the characteristic wavelength of the electrons (for example, Fermi wavelength) and Z is the distance between the centers of the wave functions in the wells, is comparable with the levels splitting energy Δ_T. Since $\Delta_T \simeq 1$–5 meV, and Z is usually larger than λ, the electron spectrum of DQW's is significantly modified when the cyclotron energy is still small in comparison with the size quantization energies ($\sim$ 50–100 meV).

Magnetic-field-induced modifications of the electron energy spectrum in DQW's change the electrical properties of this system. Recent experimental studies[4–7] of the electrical conductivity of DQW's have revealed a number of interesting features. Quenching of the resistance resonance peak (i.e., the maximum resistivity in the tunneling resonance conditions in the DQW's with nonsymmetrical scattering[8]) by the magnetic field, and anisotropy of this phenomenon with respect to the angle between the magnetic field and current have been observed.[5–7] A complex N-shape behavior of the conductivity in large magnetic fields, when the Fermi level passes through the tunnel-induced energy gap, has been found.[3,4] Although the physical reasons for these phenomena and their connection with the shape of the Fermi surface (see Fig. 1, which describes the deformation of the Fermi surface by the magnetic field) have been discussed in the cited papers, theoretical examination of the DQW's conductivity is still not sufficient. In Refs. 3 and 4 this conductivity has been calculated in the relaxation-time approximation. It is a simplified approach, which is not valid for a quantitative description of the conductivity in general, when the scattering asymmetry (asymmetrical distribution of the scatterers in the growth direction) and the long-range nature of the scattering potentials must be taken into account. In Ref. 7 the conductivity has been calculated in the limit of small magnetic fields (when ε_H is small in comparison with the Fermi energy) and expressed through the transport times. However, due to the magnetic-field-induced anisotropy of the scattering, the transport times do not describe the conductivity even in the case of small magnetic fields (see below).

In this paper we present a theory of the electrical conductivity of DQW's under the in-plane magnetic field. The conductivity tensor of the DQW's is calculated in the low-temperature limit, when the electron gas is degenerate and the most important scattering mechanism

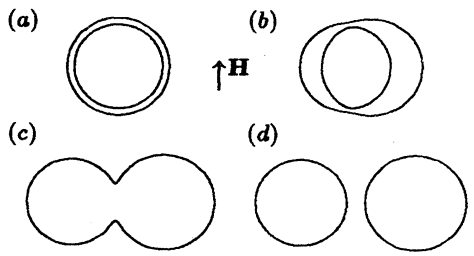

FIG. 1. Modification of the Fermi surface for a double quantum well with the increasing magnetic field $\mathbf{H}$: (a) $H = 0$, the isotropic case; (b) small H, the tunnel coupling is partly suppressed; (c) large H, the Fermi energy lies in the tunnel-induced gap; (d) very large H, the Fermi surface splits in two circles.

is the elastic scattering (due to the impurities, interface roughnesses, etc.). Calculation is done in the two-level approximation, which is valid when the cyclotron energy is smaller than the quantization energies of the electrons in the wells. Assuming that the level splitting energy is high in comparison with the collision broadening energy $\hbar/\tau$ (here τ is a typical scattering time), and the two tunnel-coupled states are well defined, we use an ordinary kinetic theory, based upon a pair of the Boltzmann kinetic equations for the distribution functions of electrons. Even in these approximations, the problem appears to be rather difficult, because both the electron energy spectrum and scattering probabilities are anisotropic, since the in-plane magnetic field is considered. For this reason, the kinetics of the momentum relaxation cannot be described by introduction of the relaxation times. In general, a numerical solution of the kinetic equations is necessary.

Below, in Sec. II, we give basic equations describing the DQW's in the in-plane magnetic field. In Sec. III we consider the scattering on the short-range correlated potentials, when the scattering probability is independent of the momentum transfer. In this model, the kinetic equations are solved exactly in the whole range of the magnetic fields. We present a general expression of the conductivity tensor, as well as its limit in the case of small magnetic fields, when ε_H is smaller than the Fermi energy, but can be comparable with the level-splitting energy. In Sec. IV we present results of the numerical solution of kinetic equations in the more general situation, when the scattering is described by a finite correlation length. We also compare our results with the experimental data. Discussion and concluding remarks are given in Sec. V.

II. GENERAL FORMALISM

In this section we describe the wave functions, energy spectrum, and group velocities of the electrons in DQW's, and derive the linearized kinetic equations and general expression of the conductivity tensor.

A. Electron energy spectrum

The electron states in the DQW's under in-plane magnetic field $\mathbf{H}$ are described by the Hamiltonian

$$\frac{1}{2m}\left(\mathbf{p}-\frac{e}{c}\mathbf{A}\right)^2-\frac{\hbar^2}{2m}\frac{\partial^2}{\partial z^2}+U(z)\ , \tag{1}$$

where $\mathbf{p}=(p_x,p_y)$ is the 2D momentum, m is the electron mass, z is the transverse coordinate, $U(z)$ is the potential energy of DQW's, e is the elementary charge, c is the light velocity, and $\mathbf{A}$ is the vector potential. Assuming that the magnetic field is directed along the y axis, and using the Landau gauge, we have $\mathbf{A}=[H(z-z_0),0,0]$, where z_0 is an arbitrary coordinate appearing due to the gradient invariance, and $H=|\mathbf{H}|$. In the further consideration, we employ a basis of the ground electron states in the l and r wells, which are described by the single-well envelope wave functions $|l\rangle$ and $|r\rangle$ (l and r orbitals). This approximation is valid when the cyclotron energy is small in comparison with the single-well quantization energies, so that the magnetic field has no considerable effect on the single-well states. In the described basis, the three-dimensional Hamiltonian (1) transforms to the 2×2 matrix Hamiltonian

$$\begin{pmatrix}\varepsilon_p+\Delta_H(p_x)/2 & T\\ T & \varepsilon_p-\Delta_H(p_x)/2\end{pmatrix}\ , \tag{2}$$

where T is the tunneling matrix element (tunnel coupling energy) and $\varepsilon_p=p^2/2m$ is the kinetic energy for the parabolic spectrum. Hamiltonian (2) is analogous to the one introduced in Ref. 9 in the absence of the magnetic field. The effect of the magnetic field on the tunnel-coupled states is described by the function $\Delta_H(p_x)$. At $H=0$ this function is equal to the level-splitting energy Δ in the absence of tunneling (the value of Δ can be controlled by application of the transverse bias to the DQW's). At $H\neq0$, $\Delta_H(p_x)$ includes additional terms, which depend of H and p_x:

$$\Delta_H(p_x)=\Delta-v_Hp_x+\delta_H. \tag{3}$$

The characteristic velocity v_H and energy δ_H are described as

$$v_H=\frac{|e|H}{mc}[\langle r|z|r\rangle-\langle l|z|l\rangle]=\omega_cZ, \tag{4}$$

$$\delta_H=\frac{m\omega_c^2}{2}[\langle l|z^2|l\rangle-\langle r|z^2|r\rangle -\langle l|z|l\rangle^2+\langle r|z|r\rangle^2]\ . \tag{5}$$

In derivation of Eqs. (2)–(5), the constant z_0 has been chosen in order to satisfy the equation $\langle l|z-z_0|l\rangle+\langle r|z-z_0|r\rangle=0$. This choice eliminates a p_x-dependent contribution appearing in both diagonal terms of the Hamiltonian (2) due to the magnetic field effect. Another symmetrical contribution in these terms (which is proportional to H^2 and does not depend on $\mathbf{p}$) is eliminated by the proper choice of the energy counting. In the symmetrical DQW's, z_0 is the coordinate of the symmetry plane. We also note that δ_H is equal to zero in the symmetrical DQW's.

Hamiltonian (2) gives rise to the electron energy spectrum

$$\varepsilon_\pm(\mathbf{p})=\varepsilon_p\pm\Delta_T(p_x)/2,$$
$$\Delta_T(p_x)=\sqrt{\Delta_H^2(p_x)+4T^2}, \tag{6}$$

where indexes "+" and "−" denote the two tunnel-coupled states, upper and lower in energy, and the function $\Delta_T(p_x)$ describes p_x-dependent splitting of these states. The group velocities $\mathbf{v}^\pm(\mathbf{p})=[v_x^\pm(p_x),v_y^\pm(p_y)]$ of the electrons in the $\pm$ states are given by

$$v_x^\pm(p_x)=\frac{p_x}{m}\mp v_H\frac{\Delta_H(p_x)}{2\Delta_T(p_x)},\ v_y^\pm(p_y)=\frac{p_y}{m}. \tag{7}$$

The wave functions of the tunnel-coupled states are described by the linear combinations[9] of the l and r orbitals,

according to $a_l^{\pm}|l\rangle + a_r^{\pm}|r\rangle$, where the projection coefficients $a_j^{\pm}$ are functions of p_x and H. In order to describe the scattering, we require the functions $\chi_{jj'}^{\pm}(p_x) = a_j^{\pm} a_{j'}^{\pm}$ describing projections of the $\pm$ states on the l and r orbitals. These functions are expressed through the DQW's parameters in the following way:

$$\chi_{ll}^{+}(p_x) = \chi_{rr}^{-}(p_x) = \frac{1}{2}\left(1 + \frac{\Delta_H(p_x)}{\Delta_T(p_x)}\right),$$
$$\chi_{rr}^{+}(p_x) = \chi_{ll}^{-}(p_x) = \frac{1}{2}\left(1 - \frac{\Delta_H(p_x)}{\Delta_T(p_x)}\right), \qquad (8)$$
$$\chi_{lr}^{+}(p_x) = -\chi_{lr}^{-}(p_x) = \frac{T}{\Delta_T(p_x)},$$

and $\chi_{lr}^{\pm}(p_x) = \chi_{rl}^{\pm}(p_x)$. We stress that the functions $\chi_{jj'}^{\pm}(p_x)$ depend on the magnetic field.

B. Kinetic equations

When the electric field $\mathbf{E} = (E_x, E_y)$ is applied along the 2D plane, the distribution functions of the electrons in the two states $f_+(\mathbf{p})$ and $f_-(\mathbf{p})$ are found from the system of two kinetic equations, which are written in the following way[10]

$$e\mathbf{E}\frac{\partial}{\partial \mathbf{p}} f_k(\mathbf{p}) = -\sum_{k'\mathbf{p}'} \mathcal{W}_{kk'}(\mathbf{p},\mathbf{p}')\left[f_k(\mathbf{p}) - f_{k'}(\mathbf{p}')\right], \qquad (9)$$

where k and k' denote $\pm$ states, and $\mathcal{W}_{kk'}(\mathbf{p},\mathbf{p}')$ is the elastic scattering probability

$$\mathcal{W}_{kk'}(\mathbf{p},\mathbf{p}') = \frac{2\pi}{\hbar}\sum_{jj'} W_{jj'}(|\mathbf{p}-\mathbf{p}'|) \times \chi_{jj'}^{k}(p_x)\chi_{jj'}^{k'}(p_x')\delta\left[\varepsilon_k(\mathbf{p}) - \varepsilon_{k'}(\mathbf{p}')\right]. \qquad (10)$$

In this equation, j, j' are the well numbers (l and r), and $W_{jj'}(|\mathbf{p}-\mathbf{p}'|)$ are the random potential correlators, whose explicit form depends upon the scattering model. For example, in the model of interface roughness scattering[11,12] we have

$$W_{jj'}(q) = \delta_{jj'} w_j \exp(-q^2 l_c^2/4\hbar^2), \qquad (11)$$

where l_c is the correlation length, which is assumed to be the same for all four interfaces, and $\delta_{jj'}$ has appeared because the roughnesses of different interfaces are statistically independent.

To calculate the linear conductivity of DQW's, we linearize the kinetic equation in the usual way,[10] by detachment of the small nonequilibrium contribution in the distribution function: $f_k(\mathbf{p}) = f_k^{(0)}(\mathbf{p}) + \Psi_k(\mathbf{p})\delta(\varepsilon_k(\mathbf{p}) - \varepsilon_F)$. Here $f_k^{(0)}(\mathbf{p})$ is the equilibrium part of $f_k(\mathbf{p})$, and ε_F is the Fermi energy, which is connected with the electron concentration n in DQW's according to

$$n = \frac{1}{\pi^2\hbar^2}\sum_k \int dp_x p_y^k(p_x), \qquad (12)$$

where we have defined $p_y^{\pm}(p_x)$ as

$$p_y^{\pm}(p_x) = \sqrt{2m\varepsilon_F \mp m\Delta_T(p_x) - p_x^2}. \qquad (13)$$

The region of integration over p_x in Eq. (12) and below is determined by an obvious requirement that the expression under the square root in Eq. (13) must be positive. We also mention the relation describing conservation of the group velocity flux through the Fermi surface

$$\int d\mathbf{p} v_x^k(p_x)\delta(\varepsilon_k(\mathbf{p}) - \varepsilon_F) \sim \int dp_x \frac{v_x^k(p_x)}{p_y^k(p_x)} = 0, \qquad (14)$$

which is valid since the Fermi surface is closed.

The electric current density $\mathbf{J} = (J_x, J_y)$ in the system is expressed through the nonequilibrium part of the distribution function:

$$\mathbf{J} = 2e\sum_{k,\mathbf{p}} \mathbf{v}^k(\mathbf{p})\Psi_k(\mathbf{p})\delta(\varepsilon_k(\mathbf{p}) - \varepsilon_F). \qquad (15)$$

The linearized kinetic equations for the functions $\Psi_k(\mathbf{p})$ are obtained after summing up Eq. (9) over p_y, using the energy conservation requirements expressed by the δ functions of energy. Such requirements imply rigid relations between p_x, p_y, and ε_F: $p_y^2 = [p_y^{\pm}(p_x)]^2$. Due to the symmetry of the electron energy spectrum with respect to p_y, it is convenient to introduce symmetrical and antisymmetrical (with respect to p_y) combinations of $\Psi_k(p_x, p_y)$, according to

$$g_k^s(p_x) = \frac{\Psi_k[p_x, p_y^k(p_x)] + \Psi_k[p_x, -p_y^k(p_x)]}{2\pi^2\hbar e E_x}, \qquad (16)$$

$$g_k^a(p_x) = \frac{\Psi_k[p_x, p_y^k(p_x)] - \Psi_k[p_x, -p_y^k(p_x)]}{2\pi^2\hbar e E_y}. \qquad (17)$$

These functions are determined from the integral equations

$$u_k(p_x) = F_k(p_x)g_k^s(p_x) - \sum_{k'}\int dp_x' R_{kk'}^s(p_x, p_x')g_{k'}^s(p_x'), \qquad (18)$$

$$1 = F_k(p_x)g_k^a(p_x) - \sum_{k'}\int dp_x' R_{kk'}^a(p_x, p_x')g_{k'}^a(p_x'), \qquad (19)$$

where the dimensionless velocity $u_k(p_x)$ is defined as $u_k(p_x) = mv_x^k(p_x)/p_y^k(p_x)$. The dimensionless kernels of the Eqs. (18) and (19) are given by

$$R_{kk'}^s(p_x, p_x') = \frac{\pi m^2}{2\hbar^2 p_y^k(p_x)p_y^{k'}(p_x')}\sum_{jj'}\chi_{jj'}^k(p_x)\chi_{jj'}^{k'}(p_x') \times \left[W_{jj'}(q_-) + W_{jj'}(q_+)\right], \qquad (20)$$

$$R_{kk'}^a(p_x, p_x') = \frac{\pi m^2}{2\hbar^2 p_y^k(p_x)p_y^{k'}(p_x')}\sum_{jj'}\chi_{jj'}^k(p_x)\chi_{jj'}^{k'}(p_x') \times \left[W_{jj'}(q_-) - W_{jj'}(q_+)\right], \qquad (21)$$

where

$$q_{\pm} = \sqrt{(p_x - p'_x)^2 + [p_y^k(p_x) \pm p_y^{k'}(p'_x)]^2}. \quad (22)$$

The function $F_k(p_x)$ is defined as

$$F_k(p_x) = \sum_{k'} \int dp'_x R^s_{kk'}(p_x, p'_x). \quad (23)$$

The linear relation between the current density $\mathbf{J}$ and electric field $\mathbf{E}$ takes form $J_x = \sigma_\perp E_x$ and $J_y = \sigma_{||} E_y$, where the components $\sigma_\perp$ and $\sigma_{||}$ of the conductivity tensor are expressed through the $g^s_k(p_x)$ and $g^a_k(p_x)$, respectively. We have

$$\sigma_\perp = \frac{e^2}{\hbar} \sum_k \int dp_x u_k(p_x) g^s_k(p_x), \quad (24)$$

$$\sigma_{||} = \frac{e^2}{\hbar} \sum_k \int dp_x g^a_k(p_x). \quad (25)$$

Let us summarize results of this section. Due to the symmetry of the 2D system in the direction of the magnetic field (y axis), the conductivity tensor is diagonal in the (x, y) coordinate system. However, the components $\sigma_\perp$ and $\sigma_{||}$ describing the currents perpendicular and parallel to $\mathbf{H}$, respectively, are not equal to each other; i.e., the magnetic field induces the anisotropy of the conductivity. Each component of the conductivity tensor is expressed through the functions $g^s_\pm(p_x)$ or $g^a_\pm(p_x)$. These functions are to be found from the one-dimensional integral equations (18) and (19), obtained after the linearization of the kinetic equations (9). In the following section we present solutions of Eqs. (19) and (20) and calculate $\sigma_\perp$ and $\sigma_{||}$ for the case of short-range scattering potentials.

III. LIMIT OF SHORT-RANGE SCATTERING

In this section we assume that dependence of the potential correlators $W_{jj'}(|\mathbf{q}|)$ of the momentum transfer $\mathbf{q}$ is not important. We also suppose that $W_{jj'}(|\mathbf{q}|)$ are diagonal with respect to the well index j:

$$W_{jj'}(|\mathbf{q}|) \simeq \delta_{jj'} w_j. \quad (26)$$

In application to the impurity scattering, this approximation means that a typical range of the single impurity potential is small in comparison with the Fermi wavelength $\lambda \sim n^{-1/2}$ and with the interwell distance Z. If we consider the interface roughness scattering, Eq. (26) means that the typical size of the roughnesses [correlation length in Eq. (11)] must be smaller than λ. We obtain

$$R^a_{kk'}(p_x, p'_x) = 0,$$

$$R^s_{kk'}(p_x, p'_x) = \frac{\pi m^2}{\hbar^2 p_y^k(p_x) p_y^{k'}(p'_x)} \sum_j w_j \chi^k_{jj}(p_x) \chi^{k'}_{jj}(p'_x). \quad (27)$$

The first equation means that the integral part of Eq. (19) vanishes. Then we have $g^a_k(p_x) = 1/F_k(p_x)$, and $\sigma_{||}$ is found in the straightforward way:

$$\sigma_{||} = \frac{e^2}{\hbar} \sum_k \int \frac{dp_x}{F_k(p_x)}. \quad (28)$$

On the other hand, the integral equation (18) with the factorized kernel $R^s_{kk'}(p_x, p'_x)$ from Eq. (27) has the solution

$$g^s_k(p_x) = \frac{u_k(p_x)}{F_k(p_x)} + \frac{C_l \chi^k_{ll}(p_x) + C_r \chi^k_{rr}(p_x)}{p_y^k(p_x) F_k(p_x)}, \quad (29)$$

where the constants C_l and C_r are determined from the system of linear equations:

$$\sum_{j'} \left[\sum_k \int dp_x \frac{\chi^k_{jj}(p_x) \chi^k_{j'j'}(p_x)}{[p_y^k(p_x)]^2 F_k(p_x)} - \delta_{jj'} \frac{\hbar^2}{\pi m^2 w_j} \right] C_{j'} = - \sum_k \int dp_x \frac{\chi^k_{jj}(p_x) u_k(p_x)}{p_y^k(p_x) F_k(p_x)}. \quad (30)$$

We stress that the determinant of this system is equal to zero [it is easy to check this statement, using the definition of $F_k(p_x)$]. Therefore, the system (30) really gives us only one linear relation between C_l and C_r. However, this feature has no influence on the conductivity because of the property given by Eq. (14). Substituting (29) into (24), and expressing C_l through the C_r, we obtain

$$\sigma_\perp = \frac{e^2}{\hbar} \left[\sum_k \int dp_x \frac{[u_k(p_x)]^2}{F_k(p_x)} - \sum_k \int dp_x \frac{u_k(p_x) \chi^k_{ll}(p_x)}{p_y^k(p_x) F_k(p_x)} \sum_k \int dp_x \frac{u_k(p_x) \chi^k_{rr}(p_x)}{p_y^k(p_x) F_k(p_x)} \Big/ \sum_k \int dp_x \frac{\chi^k_{ll}(p_x) \chi^k_{rr}(p_x)}{[p_y^k(p_x)]^2 F_k(p_x)} \right]. \quad (31)$$

Under investigation of the DQW's with high electron concentration (when $\varepsilon_F \gg T$), it is worth considering the case of small fields, when the magnetic field drives the tunnel-coupled states out of the resonance, but causes no considerable anisotropy of the electron energy spectrum. Using $u_\pm(p_x) \simeq p_x/p_y^\pm(p_x)$ and $p_y^\pm(p_x) \simeq \sqrt{p_F^2 - p_x^2}$, where $p_F \simeq \hbar\sqrt{\pi n}$ is the Fermi momentum, we rewrite expressions (28) and (31) as

$$\sigma_{||} = \frac{\sigma_0}{1-\mu^2}\left\{1 - 2\mu^2\left[I_0(H) - I_2(H)\right]\right\}, \tag{32}$$

$$\sigma_\perp = \frac{\sigma_0}{1-\mu^2}\left\{1 - 2\mu^2\left[I_2(H) - I_1^2(H)/I_0(H)\right]\right\}, \tag{33}$$

where $\sigma_0 = e^2 n\tau/m$ is the conductivity at $H = 0$ and $\Delta = 0$, which is expressed through the reduced relaxation time $\tau = 2\tau_l\tau_r/(\tau_l + \tau_r)$, where $\tau_l = \hbar^3/mw_l$ and $\tau_r = \hbar^3/mw_r$ are the relaxation times in the l and r wells. The constant $\mu = (\tau_r - \tau_l)/(\tau_r + \tau_l)$ characterizes the scattering asymmetry. In Eqs. (32) and (33) we have introduced the following functions of the magnetic field

$$\begin{aligned} I_0(H) &= \mathrm{Re}\left[\frac{1}{\sqrt{(1-iy)^2 + x^2}}\right], \\ I_1(H) &= \frac{1}{x}\mathrm{Im}\left[\frac{1-iy}{\sqrt{(1-iy)^2 + x^2}}\right], \\ I_2(H) &= \frac{1}{x^2} - \frac{1}{x^2}\mathrm{Re}\left[\frac{(1-iy)^2}{\sqrt{(1-iy)^2 + x^2}}\right], \end{aligned} \tag{34}$$

where the dimensionless parameters x and y are defined as

$$x = \frac{p_F v_H\sqrt{1-\mu^2}}{2T}, \quad y = \frac{(\Delta + \delta_H)\sqrt{1-\mu^2}}{2T}. \tag{35}$$

The rule of calculation of the square root from the complex expression $(1-iy)^2 + x^2$ in Eqs. (34) can be specified, for example, by the requirement that the result of this calculation at $y \to 0$ must be positive. Expressions (32)–(35) can be useful for interpretation of the resistance resonance shape in the in-plane magnetic field.[5,6] These expressions immediately show that (a) the quenching of the resistance resonance becomes significant when $x > 1$, or $\omega_c p_F Z > 2T$; (b) $\sigma_\perp$ always increases faster than $\sigma_{||}$ with the increase of H. Both these results are in agreement with all the experimental data and recent theoretical results.[7] At $\Delta = \delta_H = 0$ ($y = 0$), our results are consistent with Eqs. (2)–(4) of Ref. 7. In the limit $\hbar/\tau \ll 2T$, Eqs. (32)–(35) generalize Eqs. (2)–(4) of Ref. 7 for the nonresonant case, when the energy levels in the two wells do not coincide.

IV. NUMERICAL RESULTS AND COMPARISON WITH THE EXPERIMENTS

The integral equations (18) and (19) cannot be solved in general when the dependence of $W_{jj'}(|\mathbf{q}|)$ of $\mathbf{q}$ is important (scattering potentials with a finite correlation length). A common method of the solution, based on the introduction of the transport times, is valid only in the isotropic situation ($H = 0$) and fails as the magnetic field increases and the problem becomes anisotropic. In fact, the transport times do not describe the conductivity, when either the energy spectrum or scattering probabilities are anisotropic.[10] For this reason, a simple analytical solution of the kinetic equations cannot be obtained even in the case of small magnetic fields (considered in the end of the previous section), when the electron energy spectrum is isotropic, but the scattering probabilities are anisotropic due to the dependence of the overlap factors $\chi_{jj'}^\pm(p_x)$ of p_x.[13] Therefore, Eqs. (2)–(4) of Ref. 7 are valid only in the case of short-range scattering potentials ($l_c = 0$), but not in the general case. In order to describe the conductivity of DQW's in the in-plane magnetic field, it is necessary to solve the kinetic equations numerically.

Below we present results of the numerical solution of Eqs. (18) and (19) using a standard iterative procedure. In such a calculation we should restrict ourselves by some

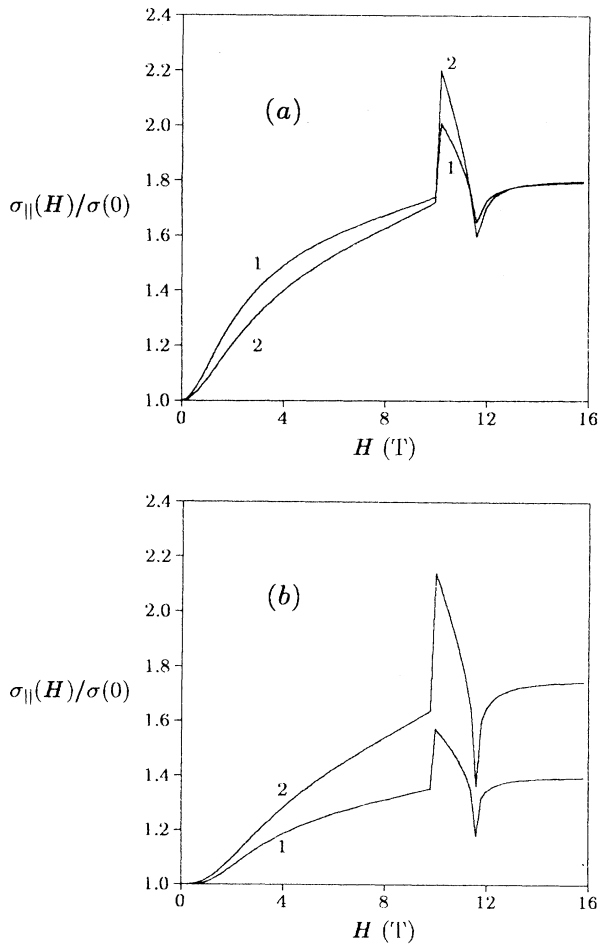

FIG. 2. Magnetic-field dependence of the conductivity $\sigma_{||}$ (configuration $\mathbf{J} \parallel \mathbf{H}$). Parameters of the structure are given in the text; 1. l_c =0, 2. l_c =10 nm; (a) $\Delta = 0$, (b) $|\Delta| = 2T$.

model of scattering. We use the model described by the correlation function (11). Although this model is not general, it describes both the scattering asymmetry (the ratio of the mobilities in the wells is given by the factor w_l/w_r), and properties of the long-range scattering potentials (finite correlation length l_c). Figures 2 and 3 show the magnetic-field dependence of the conductivity tensor components $\sigma_{||}$ and $\sigma_\perp$, calculated for the symmetrical DQW's ($\delta_H = 0$) with the interwell distance Z =15 nm, electron concentration $n = 6\times10^{11}$ cm^{-2}, resonant tunnel splitting $2T$ =3 meV, and scattering asymmetry w_l/w_r =5. Consider the resonant case ($\Delta = 0$) first. In the small magnetic fields, both conductivities increase, because the magnetic field drives the Fermi circles out of the tunneling resonance [see Fig. 1(b)]. Such an increase exists only in the DQW's with nonsymmetrical scattering. This phenomenon, known as quenching of the resistance resonance,[6] has been observed in a number of experiments. In agreement with the experimental data, $\sigma_\perp$ increases faster than $\sigma_{||}$. The increase of the conductivities becomes slower as the correlation length increases. In high magnetic fields, both conductivities show steplike growth, occurring when the higher subband (+) becomes unpopulated by the electrons (in other words, the Fermi level appears in the gap). This growth is connected with the steplike behavior of the density of states.[3,4] However, due to the anisotropy of the Fermi surface [see Fig. 1(c)], the amplitude of the step is different for different components of the conductivity tensor: $\sigma_\perp$ always jumps higher (see Appendix). With the increase of l_c, the amplitude of the step increases for $\sigma_{||}$ and decreases for $\sigma_\perp$, so that the difference between $\sigma_{||}$ and $\sigma_{||}$ becomes less pronounced. When tunnel splitting $2T$ is smaller, the amplitude of the step is smaller too. The step of the conductivities is followed by the $\vee$-like dip, which is connected with the logarithmic divergence of the density of states: the Fermi level crosses the saddle point in the energy spectrum.[3,4] The region of the magnetic fields between the step and the dip corresponds to the situation shown in Fig. 1(c). After the dip, when the Fermi surface splits into two circles [Fig. 1(d)], both conductivities increase again and go to the saturation value $\sigma(\infty) = \sigma(0)(w_l + w_r)^2/(4w_lw_r)$. We stress that $\sigma(\infty)$ is the conductivity at zero tunnel coupling, which is not surprising, because in the very high magnetic fields the coherent superposition of l and r orbitals is completely destroyed.

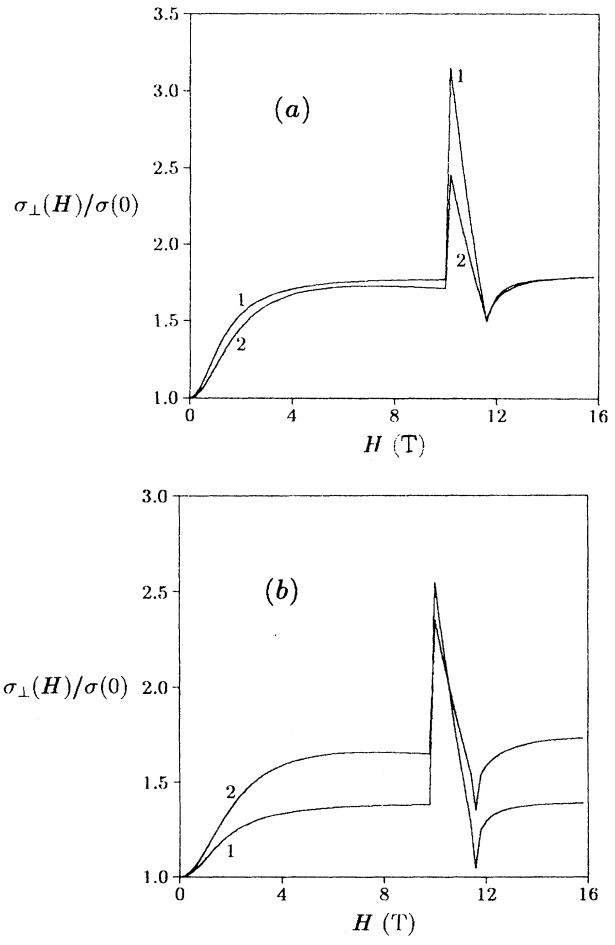

FIG. 3. The same as in Fig. 2 for $\sigma_\perp$ (configuration $\mathbf{J}\perp\mathbf{H}$).

General features described above take place at $\Delta \neq 0$, when the tunnel-coupled states are driven from the exact resonance by a transverse electric field. Application of the magnetic field also leads to the increase of $\sigma_{||}$ and $\sigma_\perp$. However, in the region of small H, this increase begins slower, because the magnetic field, driving one side of the Fermi circles from the tunneling resonance, simultaneously drives the other side towards the resonance. Moreover, at large enough $|\Delta|$, the conductivities $\sigma_{||}$ and $\sigma_\perp$ may slightly decrease with the increase of H. Experimental data[4,5] also show this behavior. In large H, both conductivities go to the same saturation value. The difference between the saturation values of the ratio $\sigma(H)/\sigma(0)$ at different l_c (in contrast to the case $\Delta = 0$) exists because $\sigma(0)$ at $\Delta \neq 0$ is smaller for larger l_c.[14]

In Fig. 4 we plot the magnetic-field dependence of $\sigma_{||}$ and $\sigma_\perp$ using experimental parameters from Ref. 4, and compared results of our calculation with the experimental data. We have chosen a single fitting parameter, the correlation length l_c, in order to make the ratio between the peaks of $\sigma_\perp$ and $\sigma_{||}$ around 7.5 T close to the experimentally observed ratio. A good quantitative agreement is obtained in the region of small magnetic fields. A qualitative agreement exists in the whole range of H. In particular, when the Fermi level lies in the gap (H = 6.8 – 8.4 T), $\sigma_\perp$ is larger than $\sigma_{||}$, in agreement with the experimental data. However, the calculated conductivities in this region are considerably larger than the experimental ones, and the latter do not show sharp steps. These discrepancies may be explained by the following. At first, the electron scattering leads to the broadening of the density of states. Also, the long-scale planar inhomogeneities (such as nonuniform doping) cause variations of the electron concentration in the DQW's plane. As a result, the sharp conductivity peaks become broadened and the amplitudes of the peaks become smaller. Other ex-

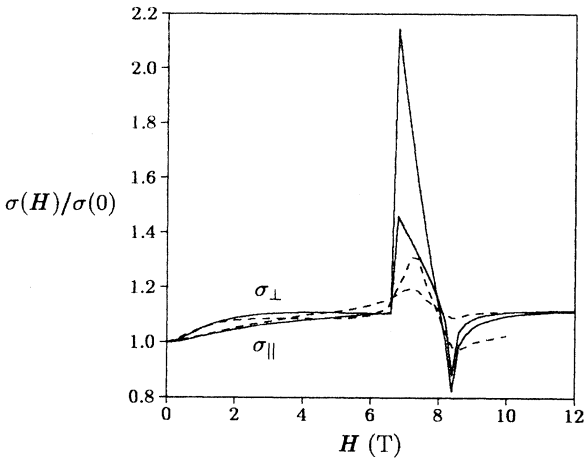

FIG. 4. Magnetic field dependence of $\sigma_{||}$ and $\sigma_\perp$ in DQW's with parameters Z =13.5 nm, $n = 2.4 \times 10^{11}$ cm^{-2}, $2T$ =1.8 meV, and w_l/w_r =2, taken from Ref. 4 ($\delta_H = 0$ since both wells have equal widths). Solid lines represent the results of calculation for $l_c = 12$ nm. Dashed lines are the experimental results (Ref. 4).

planations, such as size effects, are also possible. We also stress that the calculated peak amplitudes can be lowered if we assume that the splitting energy $2T$ is smaller than 1.8 meV mentioned in Ref. 4.

In Fig. 5 we present a comparison of our calculations with the experimental data[6] concerning quenching of the resistance resonance in the high-mobility DQW's with large mobility ratio. The value of the mobility ratio 6.7 has been obtained from the amplitude of the resistance resonance peak at H =0, and it differs from the mobility ratio 3.3 determined in condition of the full depletion[6] (possibly, due to the screening effects). We plot the magnetic-field dependence of the normalized resistivity $\Delta R/R = \sigma(\infty)/\sigma(H) - 1$. A single fitting parameter, correlation length l_c, has been chosen in order to obtain quantitative agreement with the experiment. A good agreement is achieved for both directions of **H**. However, in higher magnetic fields, the experimental points corresponding to the configuration **J** || **H** are situated above the theoretical curve, indicating that the quenching of the resistance resonance occurs slower than is expected. This discrepancy exists because our calculations have been done for the constant concentration $n = 7.5 \times 10^{11}$, which corresponds to the resonance at $H = 0$. On the other hand, the experimental data show that in high magnetic field the resonant peak for **J** || **H** is significantly shifted in the region, where the electron concentration is smaller. We cannot describe the reason for this shift in the frames of our theory (it is possibly related to the size effects). Nevertheless, the mentioned discrepancy can be explained taking into account that the quenching goes slower for the smaller electron concentration. In Fig. 5 we also show results of calculation at l_c =0 (short-range scattering potentials). Corresponding curves are situated considerably below the experimental points, indicating that the scattering on the short-range potentials was not important in the investigated[6] DQW's.

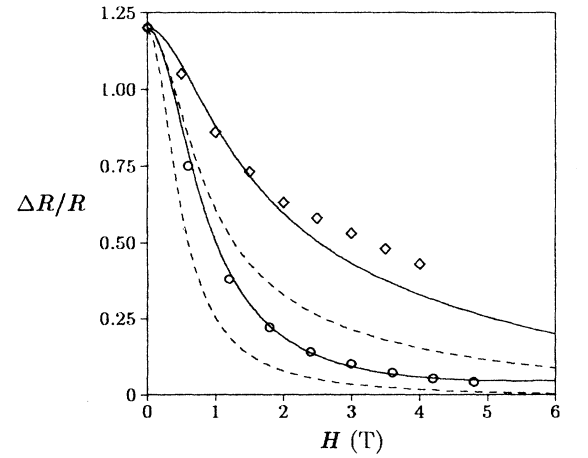

FIG. 5. Magnetic field dependence of the normalized resistivity calculated for the structure with parameters Z =17.25 nm, $n = 7.5 \times 10^{11}$ cm^{-2}, $2T$ =2.0 meV, w_l/w_r =6.7, and $\delta_H = 0$ taken from Ref. 6. Solid lines, l_c =12 nm, dashed lines, l_c =0; circles and diamonds are the experimental points (Ref. 6). Upper lines, **J** || **H**; lower lines, **J**⊥**H**.

V. CONCLUDING REMARKS

In this paper we have examined behavior of the electrical conductivity of DQW's under the in-plane magnetic field **H**. One of the most interesting features of the conductivity is its anisotropy with respect to the angle θ between the magnetic field and the current. In the most common situation, when the tunnel coupling energy is small in comparison with the Fermi energy, a significant anisotropy exists in the two distinct regions of the magnetic fields, described below. The first is the region of *high magnetic fields*, when the Fermi energy lies in the gap and the Fermi surface is described by the single anisotropic branch; see Fig. 1(c). The anisotropy of the conductivity in this region exists due to the anisotropy of the Fermi surface. On the other hand, below or above the mentioned region, the Fermi surface consists of two circles, either intersecting, or not, respectively; see Figs. 1(b) and 1(d). Each of these circles corresponds to the single well (left or right), and the scattering of the electrons in the Fermi surface occurs mostly within each circle (intrawell scattering). Since each Fermi circle is nearly isotropic, the conductivity tensor is nearly isotropic too (a small anisotropy, determined by the ratio of the tunnel coupling energy to the Fermi energy, exists in the region of H, where the Fermi circles intersect each other). Another region, where the anisotropy may be significant, is the region of *small magnetic fields*, where the tunnel coupling is not significantly suppressed by the magnetic field; i.e., the density of the electron states near the intersections (anticrossing points) is comparable with the overall density of states in the Fermi surface. The anisotropy of the conductivity in this re-

gion is connected with the anisotropy of the scattering. This anisotropy exists in the DQW's with nonsymmetrical distributions of scatterers in the direction of growth, where the resistance resonance phenomenon takes place. In other words, the magnetic field induces the anisotropic quenching of the resistance resonance.

When the angle θ is neither zero nor $\pi/2$ and $\sigma_\perp \neq \sigma_{||}$, the direction of the current is not coinciding with the direction of the applied electric field. This property gives rise to the charge accumulation phenomena in the real samples. Consider a rectangular Hall bar with the length l and width d. When the magnetic field is directed at the angle θ with respect to the bar axis and the longitudinal bias U_l is applied to the bar, a transverse bias U_t appears on the Hall contacts. The absolute value of U_t is equal to $\alpha(\theta)|U_l|d/l$, where $\alpha(\theta)$ is the anisotropy constant, which goes to its maximum at $\theta = \pi/4$:

$$\alpha(\pi/4) = \left|\frac{\sigma_\perp - \sigma_{||}}{\sigma_\perp + \sigma_{||}}\right|. \tag{36}$$

The sign of U_t is changing when we rotate the direction of **H**. Typical values of the anisotropy constant may be extracted from the experimental data. For example, the DQW's investigated in Ref. 6 had $\alpha(\pi/4) \simeq 0.14$ at H =1.2 T (small-field region). Another sample, investigated in Ref. 4, had the most significant anisotropy in the high-field region: $\alpha(\pi/4) \simeq 0.05$ at H =7.3 T.

Below we discuss the approximations used in this paper. Our calculations were based upon the Boltzmann kinetic theory, which is valid when the scattering does not suppress the coherent tunneling [it means that the minimum splitting energy $2T$ is large in comparison with the characteristic broadening energy $\hbar/\tau$]. This requirement has been fulfilled in both experiments[4,6] analyzed in this paper. To be precise, the values of $2T$ in Refs. 4 and 6 are equal to 1.8 and 2.0 meV, respectively, while the broadening energies $\hbar/\tau$ estimated with use of the mobilities in the low-mobility wells are 0.27 and 0.25 meV. On the other hand, we did not analyze experimental data from Refs. 5 and 7, because in the conditions[5,7] $\hbar/\tau$ is comparable with $2T$ and the tunnel coupling is partly suppressed due to the scattering. An examination of this case (it will be reported at a later date) requires a quantum kinetic approach. In our calculations we have neglected the spin splitting of the electron states in the magnetic field. This splitting must be taken into account when it is comparable with the tunnel splitting $2T$. However, in the $GaAs/Ga_xAl_{1-x}As$ structures, the spin splitting is small enough (less than 0.3 meV even at $H \sim 10$ T), due to the smallness of the g factor of the electrons. Another important approximation concerns the scattering model described by the correlation function (11). As a result of its usage, the validity of the numerical results presented in this paper is restricted by the proper class of the scattering potentials (interface roughnesses with the same correlation length l_c for all the interfaces). For instance, these results cannot be directly applied in the case of Coulomb impurity scattering. In spite of this restriction, the model gives a good agreement with the experimental data, when the correlation length is used as a single fitting parameter. The results of the fitting provide reasonable values of the correlation length, $l_c \sim 12$ nm, which are larger that the Fermi wavelengths in the investigated DQW's.[4,6] This fact is a confirmation that the electron scattering due to the long-range scattering potentials is important in these structures.

ACKNOWLEDGMENT

This work has been supported in part by Grant No. U65200 from the Joint Fund of the Government of Ukraine and International Science Foundation.

APPENDIX

Below we estimate the relative size of the conductivity steps corresponding to the "critical" magnetic field H_c when the subband "+" becomes unpopulated. We use a simple model of short-range-correlated scattering potentials [Eqs. (28) and (31)] and assume $\Delta = \delta_H = 0$. Since the conductivity in high magnetic fields is not very sensitive to the scattering asymmetry, we put $w_l = w_r$ for simplicity. In this case Eq. (28) gives

$$\sigma_{||}(H \to H_c) \sim \int dp_x p_y^-(p_x) \Big/ \int dp_x \left[\frac{1}{p_y^-(p_x)} + \frac{1}{p_y^+(p_x)}\right]. \tag{A1}$$

The steplike behavior of this expression is connected with the peculiar property of the following integral

$$I_c = \int \frac{dp_x}{p_y^+(p_x)} = \begin{cases} \pi/\sqrt{1+\gamma^{-2}}, & H = H_c - 0 \\ 0, & H = H_c + 0 \end{cases}, \quad \gamma = \sqrt{\frac{4T}{mv_H^2}}, \tag{A2}$$

which is also responsible for the step of the density of states. The value of γ is usually small, since the tunnel splitting is typically smaller than the Fermi energy. Calculation of $\sigma_{||}$ in the limit of small γ provides an estimate

$$\frac{\sigma_{||}(H_c + 0)}{\sigma_{||}(H_c - 0)} \simeq 1 + \frac{1}{2\sqrt{1+\gamma^{-2}}}. \tag{A3}$$

Similar calculation using Eq. (31) gives

$$\sigma_\perp(H \to H_c) \sim \left\{ \int \frac{p_x^2 dp_x}{p_y^-(p_x)} \left(1 - \frac{mv_H^2}{2\Delta_T(p_x)}\right)^2 + v_H^2 \left[\int \frac{p_x^2 dp_x}{p_y^-(p_x)\Delta_T(p_x)} \right.\right.$$
$$\left.\left. \times \left(1 - \frac{mv_H^2}{2\Delta_T(p_x)}\right)\right]^2 \Big/ \left[\int \frac{dp_x}{p_y^-(p_x)} \frac{4T^2}{\Delta_T(p_x)^2} + I_c \right] \right\} \Big/ \left[\int \frac{dp_x}{p_y^-(p_x)} + I_c \right] \tag{A4}$$

This equation shows that the step of $\sigma_\perp$ is always higher than the step of $\sigma_{||}$ due to an additional steplike contribution from the last term of Eq. (31). For small γ we obtain

$$\frac{\sigma_\perp(H_c+0)}{\sigma_\perp(H_c-0)} \simeq \frac{\sigma_{||}(H_c+0)}{\sigma_{||}(H_c-0)} \frac{1+8\gamma/[\pi^2(\sqrt{2}-1)]}{1+8\gamma/[\pi^2(\sqrt{2}-1+1/\sqrt{1+\gamma^2})]}. \tag{A5}$$

Estimating relative size of the conductivity steps with parameters used for calculation of Figs. 2 and 3, we obtain $\sigma_{||}(H_c+0)/\sigma_{||}(H_c-0) \simeq 1.15$ and $\sigma_\perp(H_c+0)/\sigma_\perp(H_c-0) \simeq 1.59$, which demonstrates significant difference between these values.

[1] T. Ando, A.B. Fowler, and F. Stern, Rev. Mod. Phys. **54**, 437 (1982).

[2] G.S. Boebinger, A. Passner, L.N. Pfeiffer, and K.W. West, Phys. Rev. B **43**, 12 673 (1991).

[3] S.K. Lyo, Phys. Rev. B **50**, 4965 (1994).

[4] J.A. Simmons, S.K. Lyo, N.E. Harf, and J.F. Klem, Phys. Rev. Lett. **73**, 2256 (1994).

[5] A. Kurobe, I.M. Castleton, E.H. Linfield, M.P. Grimshaw, K.M. Brown, D.A. Ritchie, M. Pepper, and G.A.C. Jones, Phys. Rev. B **50**, 4889 (1994).

[6] Y. Ohno, H. Sakaki, and M. Tsuchiya, Phys. Rev. B **49**, 11 492 (1994).

[7] Y. Berk, A. Kamenev, A. Palevski, L.N. Pfeiffer, and K.W. West, Phys. Rev. B **51**, 2604 (1995).

[8] A. Palevski, F. Beltram, F. Capasso, L.N. Pfeiffer, and K.W. West, Phys. Rev. Lett. **65**, 1929 (1990).

[9] F.T. Vasko, O.G. Balev, and P. Vasilopoulos, Phys. Rev. B **47**, 16 433 (1993).

[10] See, for example, B.R. Nag, *Electron Transport in Compound Semiconductors* (Springer-Verlag, Berlin, 1980).

[11] P.J. Price and F. Stern, Surf. Sci. **132**, 577 (1983).

[12] F.T. Vasko and O.E. Raichev, Phys. Rev. B **50**, 12 195 (1994).

[13] An exception is the case of DQW's with symmetrical scattering, where the phenomenon of resistance resonance is absent.

[14] Y. Berk, A. Kamenev, A. Palevski, L.N. Pfeiffer, and K. W. West, Phys. Rev. B **50**, 15 420 (1994).